

# Afterbodies and Nozzles Optimization by Using Inverse Methods

Francesco Larocca

Dip. Ingegneria Aeronautica e Spaziale, Politecnico di Torino,  
Corso Duca degli Abruzzi, 24 I-10129, Torino, Italy.

## Abstract

A numerical technique for solving design problem for 2-D and axisymmetric duct flows is presented. The method is also used to evaluate the shape of plumes and interfaces of flows with different thermodynamic properties. The unsteady Euler equations are integrated numerically by using a time-dependent procedure and by adopting an upwind finite volume approximation that belongs to the class of the the second order ENO schemes.

Several numerical examples are presented: the design of diffusers that perform transonic compression through a shock wave in the flow core, but shockless at the walls, is shown feasible; the evaluation of the shape of plumes for axisymmetric nozzles and for 2-D simple expansion ramp nozzle is also performed.

## Introduction

The efficiency of propulsion systems is strongly affected by the air intake and nozzle. Despite their quite simple geometry, such devices exhibit flow phenomena that can be rather complex over the expected range of operation.

Furthermore, in hypersonic propulsion the high integration of airbreathing engines in the vehicle requires an accurate prediction of the exhaust system performances because of its strong influence on the net thrust. For example, the flow through a single-sided nozzle can interact with the external airflow causing an increase of the installation drag, which reduces the net thrust even if the gross thrust is relatively high, specially in the transonic flight speed [1]. The description of the flow phenomena is complicated

by the presence of shear layers, due to the interaction of flows with different thermodynamic properties; the location of the interfaces are not known a priori and will be part of the solution.

The design of the compression and expansion components, the assessment of the flow behaviour through these apparatuses and its interaction with the external flow field, play a very important role in the evaluation of the net thrust.

Some useful insight for studying the above mentioned flow problems can be suggested by the inverse methods. In inverse problems the designer prescribes some flow properties and then inquires for the walls geometry that realizes the imposed flow features. In the present work a numerical method for solving inverse problem is presented. It refers to compressible, two-dimensional or axisymmetric, inviscid rotational flows governed by the Euler equations.

The basic idea consists in considering the solid boundaries of the flow field as impermeable and deformable walls along which a pressure distribution is given as design datum. The wall geometries, which are unknown and part of the solution, are evaluated by using a time-dependent process, as illustrated in [2] - [4]. In the present work, we use a finite volume formulation to approximate the solution of the hyperbolic systems of conservation laws in integral form. The main advantage of the method is related to the capability of capturing flow discontinuities correctly from a numerical point of view.

We use an upwind finite volume scheme inspired to the Godunov's Flux Difference Splitting idea [5], based on the approximate Riemann solver [6], [7]. A two-steps, predictor-corrector integration scheme that belongs to the class of the second order ENO scheme is adopted [8]. The present formula-

tion retains many of the good qualities of the previous formulations we proposed in the past [3] [9], that were based on a finite difference upwind discretization of the Euler equations. The main advantage that we preserve is the consistency of the numerical procedure with the hyperbolic nature of the time dependent Euler equations: the domains of dependence of the computed points are taken into account and are not violated by the numerical computation. The method has been checked with an analytically known solution, such as the duct confined by two streamlines of the Ringleb flow considered in [11]. The method has a straightforward extension to 3-D flows, as it has been already done in the previous formulations [4], [12].

## Numerical Method

### Governing Equations

The Euler's equations for a two dimensional or axisymmetric unsteady motion of an inviscid compressible fluid, are written in divergence form:

$$\nabla \cdot [\mathbf{V}] = -\frac{\alpha}{y} \cdot \mathbf{N} \quad (1)$$

with  $\nabla$  and  $[\mathbf{V}]$  being:

$$\nabla = \frac{\partial}{\partial t} \mathbf{k} + \frac{\partial}{\partial x} \mathbf{i} + \frac{\partial}{\partial y} \mathbf{j}$$

$$[\mathbf{V}] = \{\mathbf{U}\} \mathbf{k} + \{\mathbf{F}\} \mathbf{i} + \{\mathbf{G}\} \mathbf{j}$$

where

$\alpha = 0$  for 2-D flow and  $\alpha = 1$  for axisymmetric flow,  $\mathbf{i}$ ,  $\mathbf{j}$ ,  $\mathbf{k}$  are the unit vectors of a Cartesian frame of reference of the 3D space-time  $(x, y, t)$ , and

$$\mathbf{U} = \begin{Bmatrix} \rho \\ \rho u \\ \rho v \\ e \end{Bmatrix} \quad \mathbf{F} = \begin{Bmatrix} \rho u \\ p + \rho u^2 \\ \rho uv \\ (e + p)u \end{Bmatrix}$$

$$\mathbf{G} = \begin{Bmatrix} \rho v \\ \rho uv \\ p + \rho v^2 \\ (e + p)v \end{Bmatrix} \quad \mathbf{N} = \begin{Bmatrix} \rho v \\ \rho v^2 \\ (e + p)v \end{Bmatrix}$$

$\rho$ ,  $p$ ,  $e$ , denot density, pressure and internal energy per unit volume, respectively, while  $u$ ,  $v$  are the Cartesian components of the flow velocity. All the flow properties are normalized with respect to suitable reference values.

According to the Gauss formula, the integral of eq. (1) in a given volume  $D$  of the space-time can be written as:

$$\int_{\partial D} [\mathbf{V}] \cdot \mathbf{n} d\sigma = -\alpha \int_D \frac{\mathbf{N}}{y} d\tau \quad (2)$$

with  $\partial D$  being the boundary of the volume  $D$  and  $\mathbf{n}$  the outward normal.

Eq. (2) is approximated by a finite volume technique by discretizing the  $(x, y)$  plane by means of four sided cells whose shape depends on time.

The integration in time is carried on according to the mentioned two steps scheme. At the *predictor* step, a standard first order FDS is used: the primitive variables ( $\rho$ ,  $p$ ,  $e$ ,  $u$ ,  $v$ ) are assumed at a constant average value inside each cell. The fluxes  $\mathbf{F}$ ,  $\mathbf{G}$  are evaluated by solving the Riemann's problems pertinent to the discontinuities that take place at the cells interfaces. To this purpose, we adopted the approximate Riemann solver suggested in [6]. At the *corrector* level, the second order of accuracy is achieved by assuming a linear, instead of constant, behavior of the primitive variables inside the cells, according to the ENO concept ([8], [10]).

The resulting scheme is second order accurate in both time and space.

### The boundary conditions

The computational domain is bounded by artificial (i.e. far field boundaries) and physical contours (i.e. impermeables walls), that can be solid, as in a direct problem, flexible, as in a inverse problem, or partly solid and partly flexible. The theory of characteristics states the number of conditions to be imposed at each boundary of the computational domain.

For examples, one boundary condition is needed at impermeable boundaries; it is prompted by the physics of the problem: at a solid wall the vanishing of the velocity component normal to the wall is imposed,

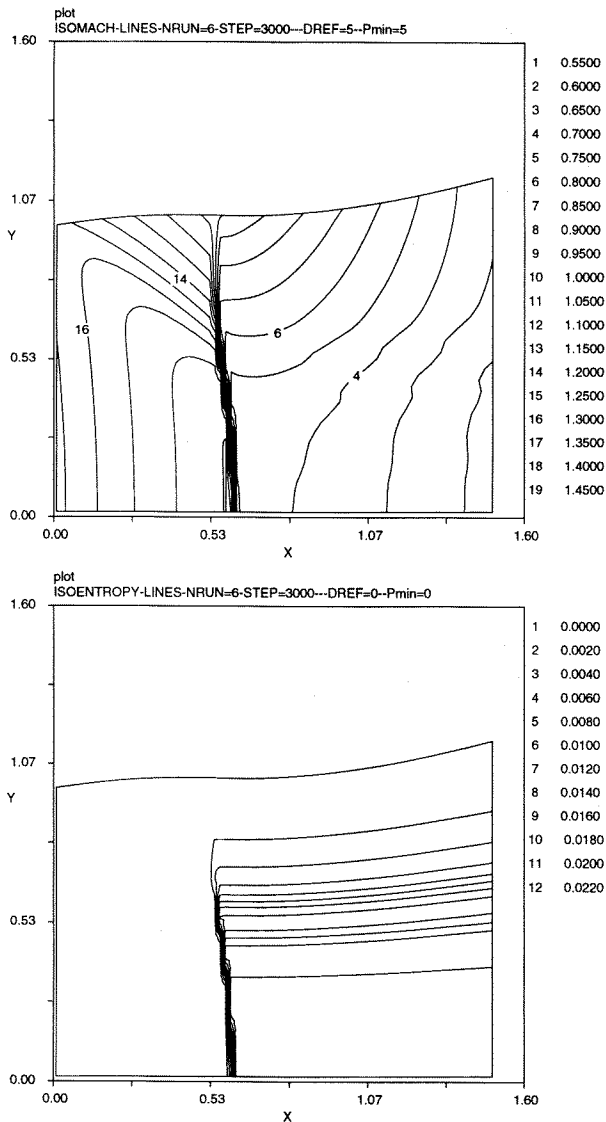


Figure 1: Transonic diffuser: a) isoMach b) isoenentropy

while at a flexible wall, according to the inverse problem formulation, the design pressure is prescribed.

The computation at the boundaries is carried out by solving an *half Riemann problem*, as described in [11].

At a deformable wall, once the flow properties are computed, the geometry is updated by enforcing the condition of impermeability: each point of the wall has to move with a normal velocity equal to the normal component of the flow velocity, as described with details in [2].

### Jet contours and interfaces

The same method here described to solve inverse problems can be used to determine the shape of plumes and interfaces. For instance, the streamtube confining a jet in air at rest can be seen as the wall of a duct along which constant pressure is prescribed.

Moreover, in flow regions, such as afterbodies or dual nozzles in by-pass turbofans, contact discontinuities are generated by different stagnation conditions and thermodynamic properties of the incoming flows. Such discontinuities are interfaces that can be computed explicitly according to the present method: they are considered as impermeable and deformable walls across which pressure and normal component of the flow velocity are imposed to be continuous.

## Numerical results

Some examples of the proposed method are here described.

The first computation refers to a transonic diffuser in which the design pressure distribution has been chosen arbitrarily; the second example deals with the design of a dual axisymmetric nozzle; finally, the flow in a single expansion ramp nozzle (SERN) with internal/external flow interactions is presented.

### 2-D transonic diffuser

In this example we look for a transonic diffuser. The design pressure along the unknown upper wall is prescribed according to the law:

$$p_d = p_{in} + dp(x/1.5)$$

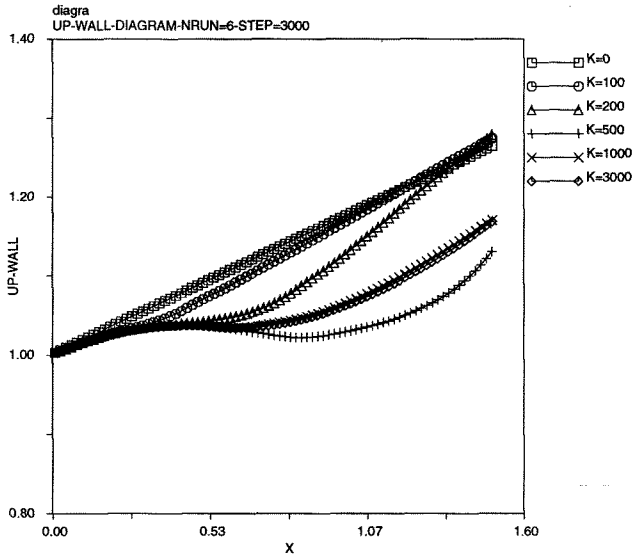


Figure 2: Transonic diffuser: wall evolution

with  $p_{in} = 0.4$ ,  $p_e = 0.75$ ,  $P^0 = 1$  and  $dp = p_e - p_{in}$

while the lower wall is assumed solid. The inlet flow is assumed supersonic, while a subsonic condition is imposed at the exit. Figs. 1 a) and b) show the final geometry with the isoMach lines and the isoentropy lines, respectively. These pictures exhibit a transition from supersonic to subsonic regime through a shock wave in the flow core but shockless at wall, as it should be expected, since the design pressure is prescribed as a continuous function along the wall.

In fig. 2 the evolution in time of the upper wall is presented. A final stable geometry is obtained even if the initial configuration ( $K = 0$ ) is very far from the final one ( $K = 1000$ ).

### Dual nozzle and contact discontinuities

In this examples we show the computation of a dual axisymmetric nozzle and jet.

The wall geometry of the external nozzle and the shapes of the interfaces confining the inner and outer flows are determined according to the inverse procedure. The computational domain is divided in two regions: the inner region which represents an "internal flow" bounded by the centerline, the inner nozzle contour and the contact discontinuity; the outer region is confined by the

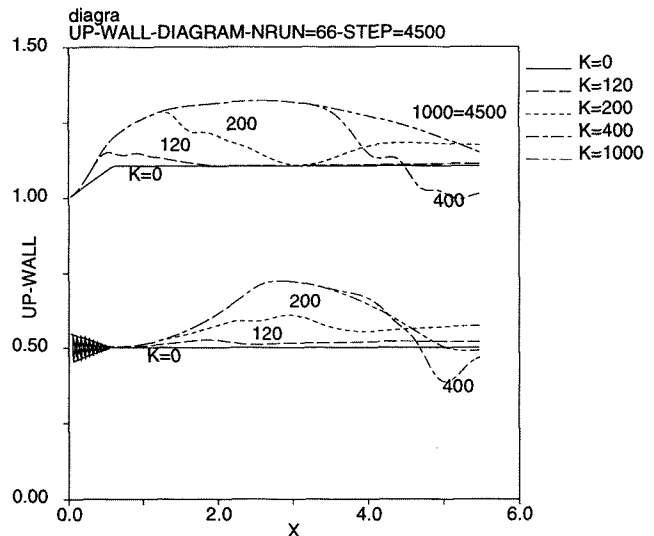
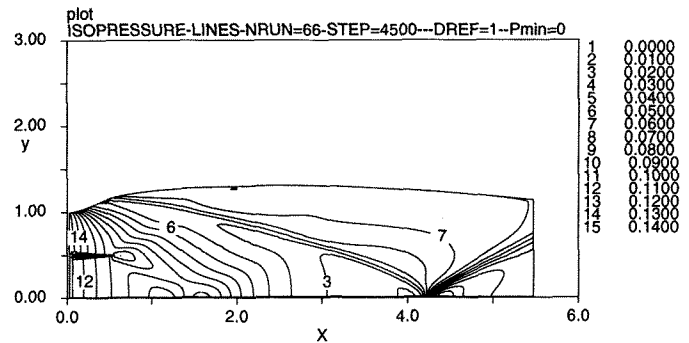
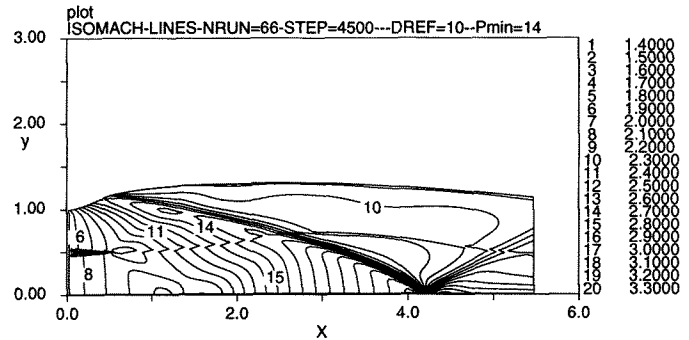


Figure 3: Dual nozzle :a) isoMach , b) isopressure c) time evolution

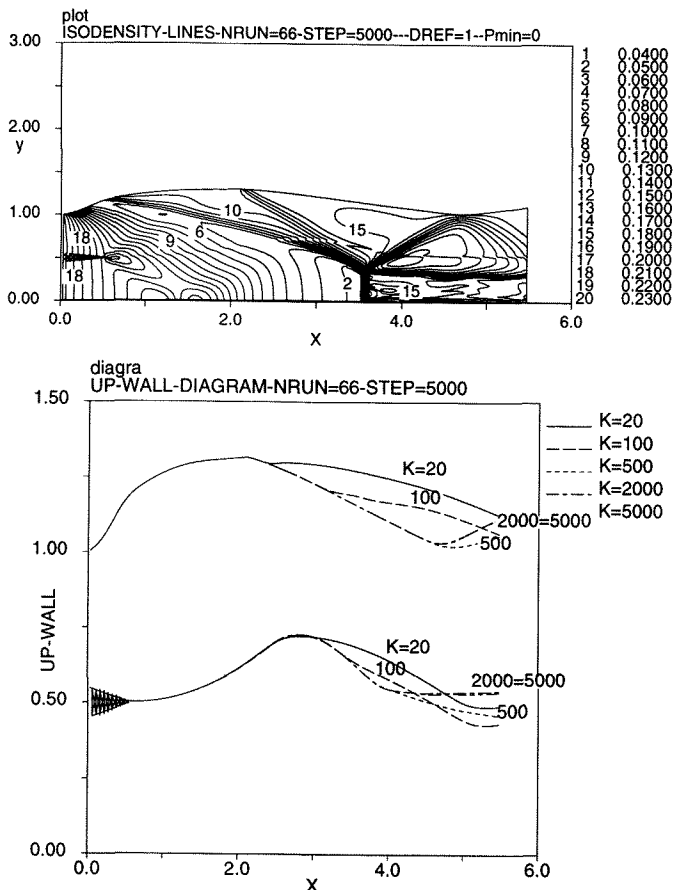


Figure 4: Dual nozzle :a) isoMach ,b) time evolution

external nozzle's walls, the contact discontinuity and a free pressure boundary. Along the outer jet contour we prescribe constant pressure  $p_e$  while along the inner contact discontinuity we impose that pressure and normal component of velocity have to be continuous across it.

The inner nozzle has a  $5^\circ$  half-angle, while the external one has a  $10^\circ$  divergence angle. The inlet flow is supersonic for both nozzles, but with different total conditions. At the inner nozzle we prescribe total pressure  $P^0 = 1.0$ , total temperature  $T^0 = 1.0$  and Mach number  $M = 2.0$ ; at the inlet of the external nozzle we impose  $P^0 = 0.9$ ,  $T^0 = 1.0$  and  $M = 1.8$ . The external pressure is  $p_e = 0.07$ .

Moreover, along the upper wall of the secondary nozzle, a design pressure distribution is set according to:

$$p_d = (p_{in} - p_e) \sin(\pi x / 1.5) \quad (0.0 < x < 1.50)$$

$$p_d = p_e \quad (1.5 < x < 2.15)$$

where  $p_{in} = 0.1566$  and  $p_e = 0.07$  are the inlet and the external pressure, respectively.

The above pressure distribution allows the secondary nozzle to be fully expanded with a nearly uniform axial flow at the exit section.

The resulting flow configuration and the geometry of the wall of secondary nozzle are shown in figs. 3. The isoMach contours, plotted in fig. 3 a), reveal the presence of an oblique shock wave due to the change of the curvature of the wall; the picture displays also the computed free pressure boundary and the shape of the interface discontinuity. In fig. 3 b) the isopressure contours show a continuous behavior across the interface.

The evolution in time of the jet contour and interface are given in fig. 3 c). The computation starts by assuming straight lines for the jet and the interface ( $K = 0$ ). The final steady configuration is obtained after  $K = 1000$  time steps.

The behaviour of the dual nozzle, with the design geometry previously computed, has been analyzed in an off-design overexpanded configuration. The inlet conditions are unchanged, while the external pressure is  $p_e = 0.1$ . The resulting flow configuration, shape of the jet contour and internal interface are shown in figs. 4.

The isodensity contours, plotted in fig. 4 a), show an inner embedded shock and a shock originated at the trailing edge of the outer nozzle; they merge generating a Mach disk, a contact discontinuity and a reflected shock that impinges on the free pressure boundary and is reflected back as an expansion wave. The isolines in this picture put also in evidence the computed shapes of plume and inner interface. The evolution in time of the jet contour and the interface are given in fig. 4 b). The flow configuration at design condition has been chosen as starting condition ( $K = 0$ ) for the off-design computation. The final steady solution has been obtained after  $K = 2000$  time steps.

### SERN nozzle

The last numerical example refers to the SERN nozzle reported in figures 5, 6. The supersonic ramp of the nozzle has been designed by using the method of characteristics at design conditions corresponding to the flight Mach number  $M = 4.0$ . The length of the ramp is 60% of the length of the ideal fully expanded nozzle.

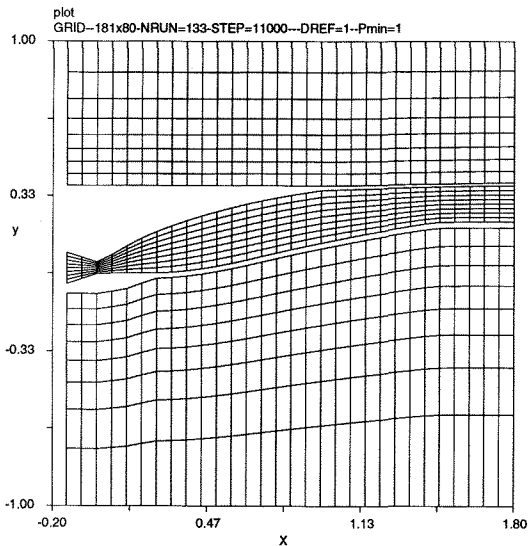


Figure 5: SERN nozzle: mesh every 6 (x) and 3 (y) grid lines

The flow computation is based on different stagnation conditions for the external air-flow and the expanding gas; it refers to an overexpanded configuration corresponding to the flight Mach number  $M = 2.0$ . The total nozzle inlet conditions, normalized with respect to the total flight condition, are given by:

$$P_{noz}^0 = 3.06 \quad T_{noz}^0 = 6.43$$

The external pressure is  $p_e = 0.1278$ . The calculations have been carried out by considering perfect gas with constant specific heat pressure ratio without accounting for real gas effects.

The flow field is composed of three domains: one is confined by the 2-D nozzle and the plume boundaries, the other are represented by the two external regions of supersonic flow. The interactions between the external flow and expanding gas give rise to shear layers which are treated as moving interfaces. In fig. 5 the computational mesh relevant to the final configuration is shown; the grid lines fit the interfaces and display the three regions. The contact discontinuities that separate the different domains are clearly detected in 6 a), where the Mach number isolines are drawn. In the lower external region an oblique shock wave originates from the flap trailing edge. It is due to the mismatch of the static pressure at the end of the flap and it is weakened by inter-

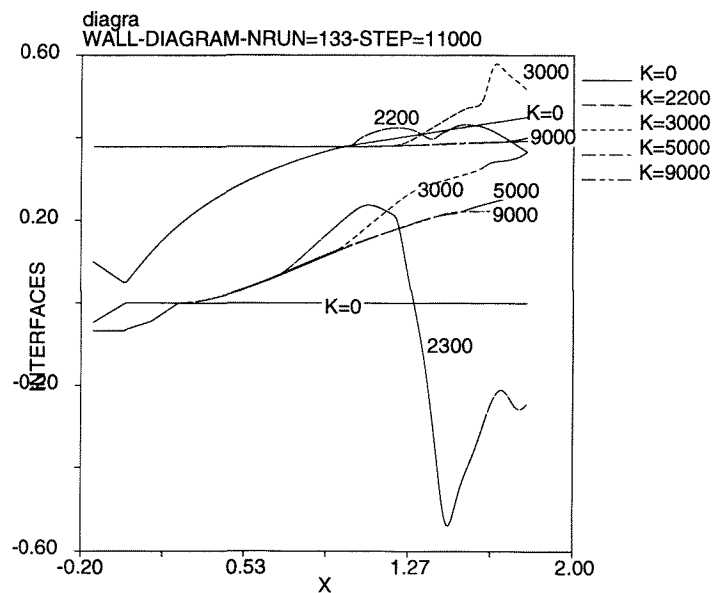
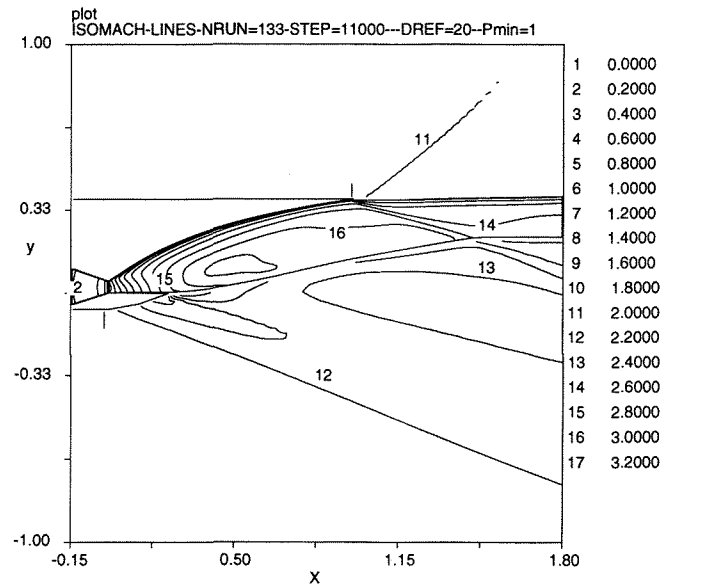


Figure 6: SERN nozzle : b) isoMach c) time evolution

acting with the expansion generated by the outer flap wall.

In the exit region, the internal flow exhibits a oblique shock wave, due to the low nozzle pressure ratio, which interacts with the plume boundary.

Finally the time evolution of the jet contours is shown in fig. 6 b). At the beginning of the computation ( $k = 0$ ) two straight lines are assumed as interfaces separating the different flow domains. At the steady solution obtained after 9000 time steps, the shapes that the interfaces assume are very far from the initial configuration.

## References

- [1] D.J. Dusa *Exhaust Nozzle System Design Considerations for Turboramjet Propulsion Systems*, IX ISABE, Sep. 1989, Athens, Greece
- [2] L. Zannetti *Time Dependent Method to Solve Inverse Problems for Internal Flows*, AIAA J., Jul. 1980, pp. 754-758.
- [3] L. Zannetti, M. Pandolfi *Inverse Design Technique for Cascades*, NASA CR 3836, Nov. 1984.
- [4] L. Zannetti, T. T. Ayele, *Time Dependent Computation of the Euler Equations for Designing Fully 3D Turbomachinery Blade Rows, Including the Case of Transonic Shock Free Design*, AIAA 25th Aer. Sp. Scien. Meet., AIAA-87-0007.
- [5] S. Osher, F. Solomon *Upwind Difference Schemes for Hyperbolic System of Conservative Laws*, Mathematics of Computation, vol. 38, 1982.
- [6] M. Pandolfi *A Contribution to the Numerical Prediction of Unsteady Flows*, AIAA J. N. 5, vol. 22, 1984.
- [7] F. Larocca, L. Zannetti *Design of Air Intakes and Nozzles for Transonic Rotational Flows*, 11th ISABE, Sep. 1993, Tokyo, Japan.
- [8] Harten et alii, J. Comput. Phys. 71 (1987), 231.
- [9] L. Zannetti, F. Larocca, *Time Dependent Euler Solution of Multidimensional Inverse Problems*, 2nd Int. Conf. on Inverse Design Concept Optimization in Engineering Sciences, University Park, Pen. Oct. 1988.
- [10] A. Di Mascio, B. Favini *A Two Step Godunov-Type Scheme for the Euler equations*, Meccanica, Vol. 26, N. 2/3, 1991, pp.179-189.
- [11] F. Larocca, L. Zannetti *Design Methods for 2-D Transonic Rotational Flows*, AIAA Paper 95-0648, Jan. 1995.
- [12] L. Zannetti, F. Larocca, *Inverse Methods for 3D Internal Flows*, AGARD-FDP-VKI Special Course , 14-18 May 1990.